

An UHF RFID tag characterization methodology including a low-cost and low-complexity SDR platform for information extraction

Juan Sebastián Moya Baquero^{1,2}, Fabian L. Cabrera¹, and Fernando Rangel de Sousa¹

¹LRF/UFSC, Universidade Federal de Santa Catarina, Florianópolis, Brasil

² Integrated Syst. Res. Group Onchip, Universidad Industrial de Santander, Bucaramanga, Colombia
e-mail: juan2178217@correo.uis.edu.co

Abstract— RFID concepts have been evolving for more than fifty years, nevertheless it was until the last decade that this technology settled as one of the leading commercial solutions being applied on, for example tracking, access management and document registration applications, among others. This technology has brought many benefits to the users, like auto-mation processes, inventory time reduction and information transmission reliability. However, before commercializing the RFIDs, test and characterization procedures must be executed in order to provide the correct information to the user. Unfortunately, lack of characterization methodology standards, high cost and high-complexity test equipment are recurrently disadvantages. This work presents an RFID characterization methodology that uses a low-cost and handy RF signal platform for Electronic Product Code (EPC) time extraction.

Index Terms—RFID Characterization, RFID Test Methodology, Software-Defined Radio, GNU-Radio, Instrumentation.

I. INTRODUCTION

RFID technology solutions have increased considerably during the last years, due to low cost and easy-to-use characteristic. Object, people and animal tracking or store inventory time-reduction are some of the most common applications. An RFID system is composed by a reader and a tag, where the operation principle is based in two requirements:

1) The reader transferred energy must be sufficient to turn-on the tag circuit.

2) The tag extracted information must be received correctly by the reader. Once these two conditions are fulfilled, an energy-information exchange takes place between both parts and then, the identification can be done by the user [1]-[4].

Before the tag becomes a commercial device, a characterization procedure shall be done to evaluate the tag performance and determine if the specifications are achieved [5]-[7]. Nevertheless, there is a lack of standard characterization methods for commercial RFID tags in Near-Field, as indicated in [8], hindering the characterization step. Moreover, the RFID tag low prices are not reflected for test equipment during the RFID Tag test and characterization phase.

Nowadays, commercial test equipment are very expensive and laboratories with reduced budget cannot afford or purchase it. For example, high frequency oscilloscope prices provided by Tektronix [9] can oscillate between 10,000 USD and 41,000 USD. Another example, corresponds to the

National Instruments proposed platform to test RFID tags, as presented in [10]. Despite its high accuracy, the platform cost exceeds several tens of thousands of USD.

This work presents a tag characterization methodology through different domains in order, to extract the information fixed in the tag. For time domain extraction, it is used a solution previously reported in [11]– [16], with low-cost, flexibility and high-accuracy characteristics. The solution corresponds to an open source Software-Defined Radio (SDR) platform for RF signals acquisition. The UHF RFID tag was designed for the Near-Field bio-medical applications and fabricated using the GF180nm CMOS process from GlobalFoundries.

The fully-integrated Tag is described in the next section, the resonator parameter extraction is presented in Sec. III, followed by the discussion of the corresponding frequency domain characterization in Sec. IV and the time domain information extraction results using the SDR platform in Sec. V. Finally, the work is concluded in section VI.

II. INTEGRATED TAG

A miniaturized full-custom integrated tag with information bit sequences fixed inside a ROM memory was designed in a standard 180 nm CMOS technology, as reported in [17]. It is delimited in a 1.5 mm×1.5 mm area for radio frequency object identification in biomedical environments. The corresponding specifications are presented in Table 1.

Table 1. Tag Specifications

Specification	Value
Load Supply Voltage	1 V
Nominal load average power	1 μ W
Carrier Frequency	1.04 GHz
Modulating frequency	1 MHz @ 1 V

A. Tag Block Diagram and functional description.

An RF/dc front-end, as presented in Fig. 1., is implemented in order to transform the magnetic flow across the inductor into a dc voltage to feed the load (dashed line). It is compo-

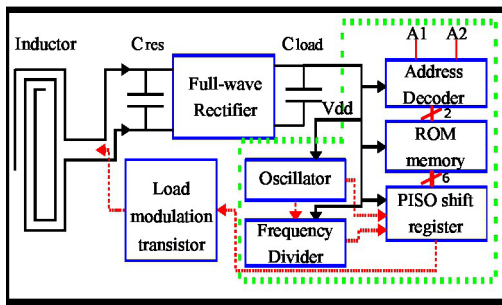


Fig. 1. Tag block diagram.

sed by a 2 nH integrated inductor, a 12 pF resonance capacitor C_{res} , a full-wave rectifier and a load capacitor C_{load} for energy storage and filtering. The tag's information bits (EPC) are stored in a full-custom NOR type ROM memory. For memory bit extraction, a Parallel-Input Serial-Output (PISO) shift register is used to transform the parallel memory bits into a bit sequence, for later load modulation and consequently, send back the information to the reader. Furthermore, the PISO shift register is a sequential logic block that uses the oscillator output as the reference control signal to avoid bit losses during the serial transformation. A frequency divider output is used to distinguish shift and load operations of the memory bits inside the PISO shift register.

Finally, the bit sequence controls a NMOS transistor gate to send back the information fixed inside the ROM memory. The solid and dashed arrows correspond to energy and information signals, respectively. Additionally, an address decoder is used to access four different bit sequences stored inside the ROM memory to increase the results quantity. Table 2 presents the memory bit sequences according to the Address Decoder inputs (A1 and A2) combinations.

Table 2. Address Bit words table.

A1	A0	Word Sequence
0	0	110101
0	1	110001
1	0	101111
1	1	101101

B. Manufactured tag

The corresponding fabricated tag is presented in Fig. 2.

In this figure, the three pads correspond to the two address decoder inputs (A1 and A2) and its corresponding ground.

All the load supply-routes are connected in star configuration in order to reduce induced current loops that can interfere with the magnetic flow passing across the inductor.

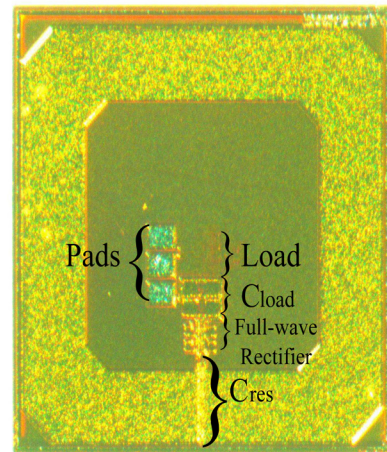


Fig. 2. Fabricated Die.

III. RESONATOR EXTRACTED PARAMETERS

Forty samples were sent back by the manufacturer. The first test implemented corresponds to the resonator parameter extraction, using the methodology described in [19]. The parameters are obtained by comparison of the extracted S11 parameter results when the tag is placed above the primary inductor and when the tag is removed. However, it was identified that a scribe line remaining, named seal ring, around the die reduces the tag inductor quality factor. Thus, the seal ring was broken by mechanical polishment. In total, the seal ring break process was executed in seven samples.

About the measurement procedure, the corresponding Open-Short-Matched (OSM) vector network analyzer (VNA) calibration technique was implemented to compensate the cables losses.

The setup is composed by three main components: the tag, the primary inductor and the two-port R&S@RZVB8 VNA. The VNA-inductor connection was made by using a semi-rigid NMD testing cable and an RA U.FL to SMA cable. The primary inductor corresponds to a 35 μm thickness one-turn copper antenna printed on an FR4 substrate with a dielectric constant of 4.4, a loss tangent of 0.02, a thickness of 1.6 mm and its value is 4.13 nH.

The corresponding experimental setup is presented in Fig. 3. A -10 dBm VNA power was set, which is sufficiently low to only energize the resonator and not its active circuitry.

The S11 parameter measurements of the tag with the seal ring intact (solid line) and cut (dashed line) are visualized in Fig. 4. It can be noted a considerable difference between both S11 results. The three parameters extracted are the resonance frequency, the integrated inductor quality factor and the inductive coupling factor. The extraction methodology was implemented in all the seven cut samples. The obtained parameter mean values are presented in Table 3.

Table 3. Parameter mean values.

Parameter	Mean Value
Resonance Frequency [MHz]	983.79
Integrated resonator quality factor	19.13
Magnetic coupling factor	0.2488

Based on the results presented in Table 3, it can be observed a shift in the resonance frequency due to process variations during die manufacturing. Additionally, the broken-seal ring integrated resonator quality factor value, 19.13, doubles approximately the extracted quality factor using the intact tag (nearly 10). Finally, a 0.2488 magnetic coupling factor mean value was achieved, indicating a strong coupling between both inductors.

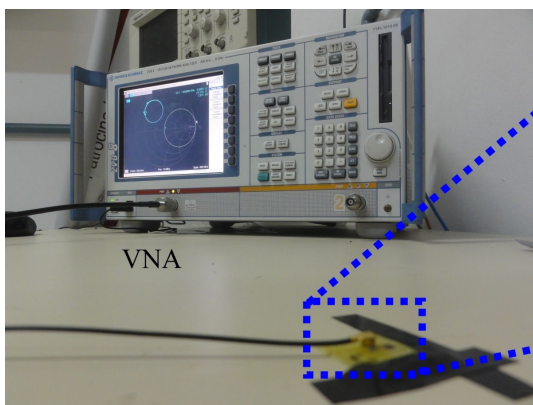


Fig.3. Experimental Setup for resonator parameter extraction.

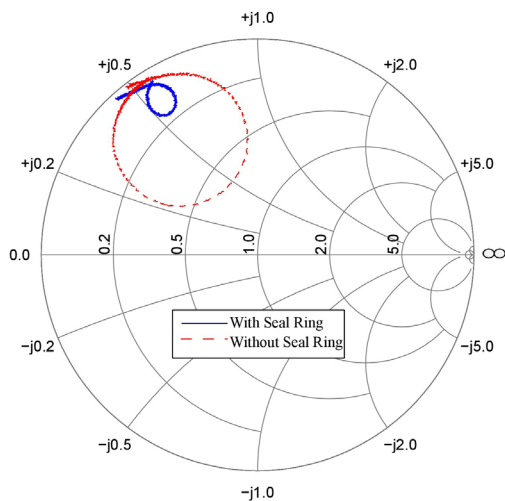


Fig.4. Smith Chart S11 results with and without seal ring.

IV. FREQUENCY DOMAIN RESULTS

Once the resonator parameters were extracted, a frequency domain test was implemented, in order to identify if the tag was sending the information. For this, the setup diagram

presented in Fig. 5 was used. In this figure, the signal generator delivers the power to the reader inductor, in order to energize the tag. Once the tag sends back the information, the modulated signal is visualized in the Spectrum Analyzer. All the energy and information signals are regulated through the power circulator, in order to control the energy direction for attenuate undesirable power reflections that can affect the measurements and the devices.

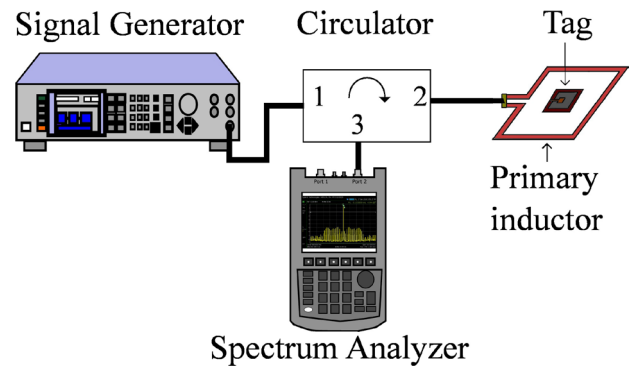


Fig.5. Frequency domain setup diagram.

The corresponding experimental setup is presented in Fig. 6. In this figure, the generator delivered power was increased gradually in order to identify the minimum power that switches-on the tag. The primary inductor used is a 35 μm thickness one-turn copper antenna printed on an FR4 substrate with a dielectric constant of 4.4, a loss tangent of 0.02, a thickness of 1.6 mm and its value is 9.4 nH.

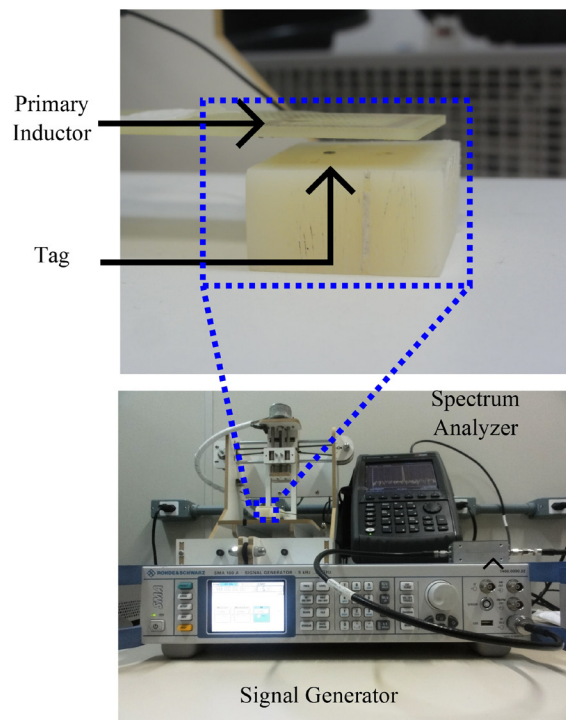


Fig.6. Frequency domain experimental setup.

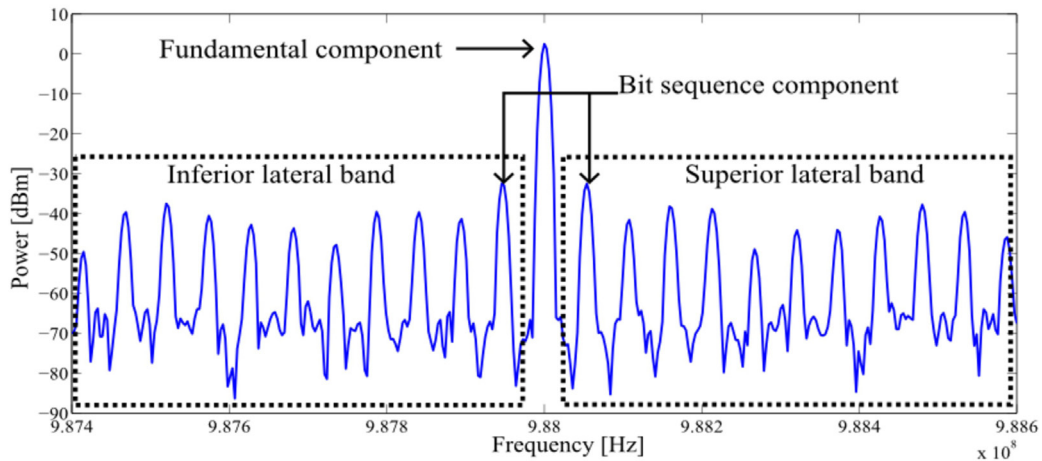


Fig.7. 18 dBm generator delivered power frequency response.

In Fig. 7, it is shown the waveform obtained for 18 dBm signal generator power for a 2 mm air-gap between the inductors. It was used a 1.2 MHz frequency-span and a 20 dB signal attenuation as a safety procedure for the Spectrum Analyzer. In this figure, the component associated to the carrier frequency signal is centered in 988 MHz with the corresponding modulating signal components (Bit sequence components) on both lateral bands. The other components obtained correspond to modulating harmonics.

Finally, in Fig. 8, it is presented the difference between the fundamental and modulating signal components for several power and distance conditions.

Based on the results presented in Fig. 8, a 12 dBm minimum power delivered by the signal generator was achieved for a 1 mm distance. For the maximum distance case, a 26 dBm delivered power was identified when there is a 15 mm air-gap between both inductors.

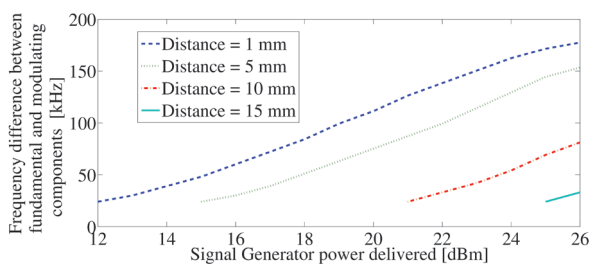


Fig.8. Frequency difference between the fundamental and modulating components for different distances and reader delivered powers.

V. TIME DOMAIN RESULTS

Once the RFID alive test was executed successfully, the next step corresponds to the information extraction. For time domain information extraction, the reader board used corresponds to the Universal Software Radio Peripheral (USRP) B210 RF signal platform [20]. A low-cost Software Defined Radio (SDR) platform that covers the 70 MHz-6 GHz fre-

quency range with two ports for transmission and two ports for reception. This platform transfers as close as possible the software domain to the antenna for reduce as much as possible hardware issues, as interconnectivity and matching. Furthermore, both frequency and power can be reprogrammed by the user and its cost oscillates between 1,000 USD and 1,700 USD.

The platform can be programmed by a free and Open-Source toolkit Gnu Radio [21], that uses a framework for design, simulation and implementation of real radio systems. In this paper, the programming is done by creating a flowgraph composed by standard library blocks, as it is presented in Fig. 10. Nevertheless, C++ and Python programming are also possible.

After defining and programming the platform as a receiver, the USRP B210 is incorporated to a time domain setup for information extraction, as presented in Fig. 9.

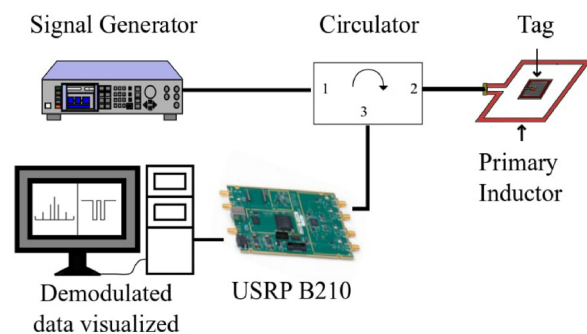


Fig.9. Time domain setup diagram with SDR platform.

The time domain setup is composed by six main components: signal generator, power circulator, primary inductor, tag, USRP B210 and a general-purpose computer. The signal generator delivers the power to the reader, whom energizes the tag for information extraction. Once the bit sequence is sent back from the tag, it is acquired, demodulated and processed by the USRP B210 RF signal platform for later visualization.

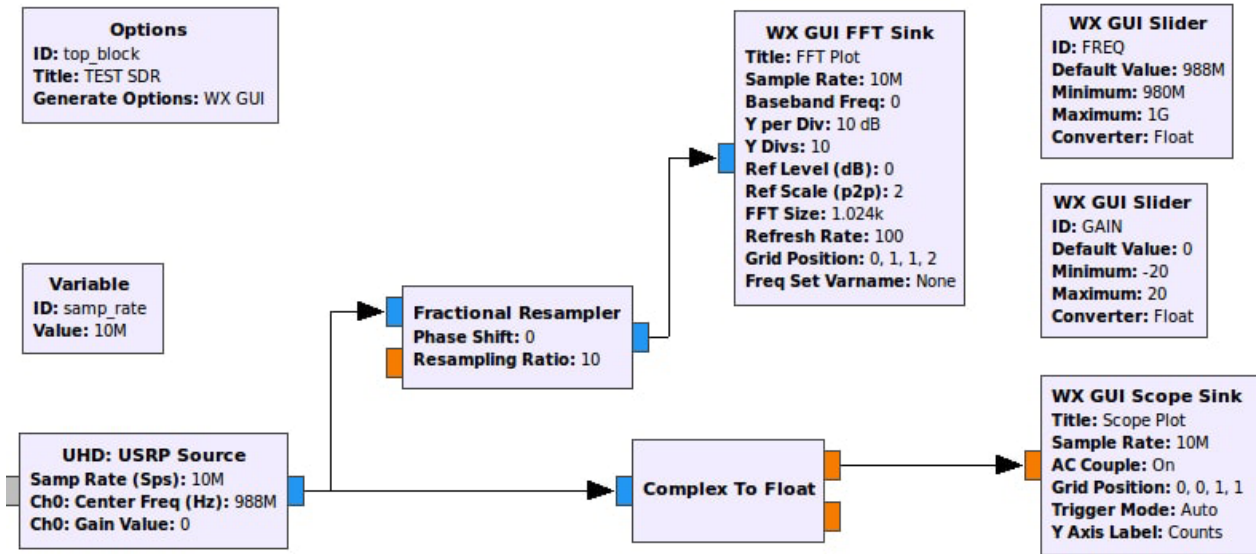


Fig.10. Flowgraph block diagram in GNU Radio

For visualizing the bit sequence, the platform is programmed by creating a flowgraph that samples the acquired information. Fig. 10 presents the flowgraph used for information demodulation and extraction. It is mainly composed by two branches, the first one allows the frequency domain visualization (Fractional Resampler and WX GUI FFT Sink blocks) and the second one implements the time response (Complex to Float and WX GUI Scope Sink blocks).

The sample rate used to visualize the information in both frequency and time domain is 10 Mbps and the local oscillator frequency to transform the information to base-band is 988 MHz. Besides this, two slider blocks were included to manipulate both local oscillator frequency and receiver amplifier gain to simplify the user control.

The corresponding experimental setup with all the components previously described is presented in Fig. 11.

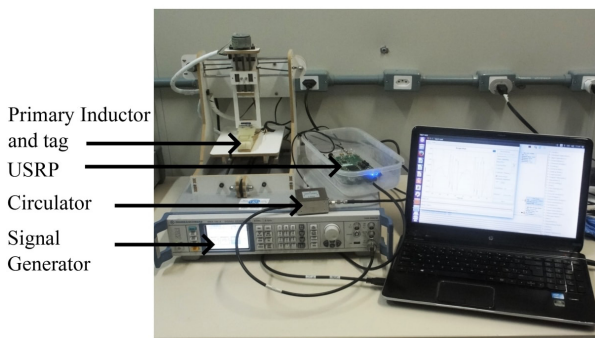


Fig.11. Time domain experimental setup with SDR platform.

The primary inductor used in this setup is the same utilized for the frequency domain results. The received, demodulated and processed information is visualized in Fig.

12. Three time-domain waveforms at different points of the reader setup are presented in Fig. 12. The graph (a) presents the data acquired using the Gnu Radio flowgraph block diagram. As it can be seen, the data obtained by the SDR platform has small amplitudes (μV order) due to the air-channel and cable receiver attenuation. Therefore, a post-processing step is needed in order to obtain the expected bit sequence.

First, data amplification is implemented in order to obtain higher voltage values and then a threshold value is set for distinguishing between high and low logical values. Both amplification and bit sequence recovery are presented in graphs (b) and (c), respectively. For this test, the bit sequence extracted was 110101, corresponding to the A0=0 and A1=0 inputs combination.

CONCLUSION

This work presented a low-cost and low complexity platform for RFID tag characterization and time domain information extraction. The test methodology of a full-custom integrated tag was discussed. Post manufacturing processes, frequency and time domain characterizations were implemented in order to determine the tag performance and information extraction.

Additionally, the seal ring influence in the extracted S11 parameter, hence, in the tag quality factor was detected and corrected manually. This allowed utilizing a validation methodology for parameter extraction of the inductive coupling link and a reduction of its turn-on power in order to minimize the reader power for information detection and proper extraction.

Once the experimental resonance frequency was identified by the parameter extraction step, 988 MHz, a frequency domain setup was implemented for detecting if the tag was

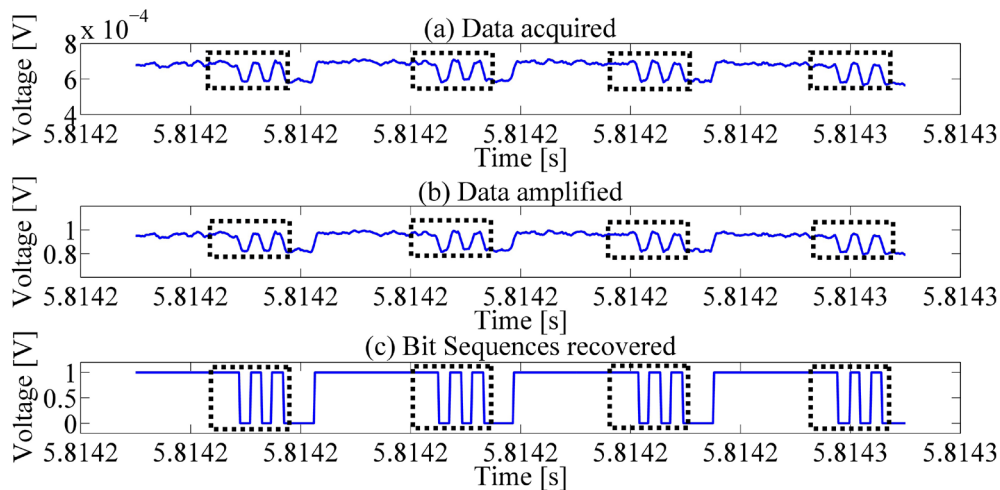


Fig.12. (a) Data acquisition, (b) amplification and (c) conversion to digital bit sequences.

alive. The obtained results showed bit sequences components on both inferior and superior bands of the fundamental component with its corresponding harmonics. A minimum 12 dBm generator delivered power was achieved for a 1 mm distance between the reader inductor and the tag. A maximum 15 mm distance was achieved with 26 dBm generator power.

Moreover, this test allows the identification of the minimum power delivered by the power generator that needs the Spectrum Analyzer to recognize the data sequence extracted from the tag.

The SDR platform together with the programming Open-Source toolkit reduce as much as possible the hardware problems by transferring the software domain closely to the receiver antenna. Its handy interface lets the user to program the extraction setups in an easy and agile way by using flowgraph diagrams as presented in this work. Data acquisition was implemented by using only three simple blocks during the programming phase. Consequently, information processing was realized by amplifying and converting to digital bit sequences.

ACKNOWLEDGEMENTS

This work was partially supported by CNPq, INCT NAMITEC and CAPES.

REFERENCES

[1] K. Finkenzeller, *RFID Handbook, Fundamentals and Applications in Contactless Smart Cards and Identification*, Second Edition. John Wiley and Sons, 2003.
 [2] H. Lehpamer, *RFID Design Principles*, Artech House Inc., 2008.
 [3] Hao Jiang et al., "RFID circuit design with optimized cmos inductor for monitoring biomedical signals.", in *15th International Conference on Advanced Computing and Communications*, 2007, pp. 203-208.
 [4] A. Baldi, et al., "Powering of single-chip fully integrated RFID wireless sensors", in *37th Annual Conference on IEEE Industrial*

Electronics Society (IECON), 2011, pp 3528-3532.
 [5] P. Nikitin et al., "UHF RFID Tag Characterization: Overview and state-of-the-art", *Intermec Technologies Corporation*, 2014, pp.1-6.
 [6] A. Soares Boaventura and N. Borges Carvalho, "A Measurement Strategy for Test and Characterization of UHF RFID Systems", in *79th Microwave Measurement Conference (ARFTG)*, 2012, p.p 1-3.
 [7] R. Colella et al., "Improved RFID Tag Characterization System: Use Case in the IoT Arena" in *IEEE International Conference on RFID Technology and Applications*, 2016, p.p 172-176.
 [8] A.C. de Souza et al., "Normalized Power Calculation to UHF RFID Passive Tags Characterization", in *IEEE Brasil RFID*, 2014, pp.54-56.
 [9] "Tektronix: Test and Measurement Equipment", <http://www.tek.com/> (Webpage accessed in 18/11/2016).
 [10] National Instruments, "Using National Instruments Software and Hardware to Develop and Test RFID Tags", <http://sine.ni.com/cs/app/doc/p/id/cs10511> (Webpage accessed in 23/11/2016).
 [11] G. Vannucci et al., "A Software Defined Radio System for Backscatter Sensor Networks", in *IEEE Transactions on wireless communications*, vol. 7, no. 6, June 2008, pp.2170-2179.
 [12] L. Catarinucci et al., "Performance Analysis of Passive UHF RFID Tags with GNU-Radio", in *IEEE International Symposium on Antennas and Propagation (APSURSI)*, 2011, pp.541-544.
 [13] L. Catarinucci et al., "A Cost-Effective SDR Platform for Performance Characterization of RFID Tags", in *IEEE Transactions on Instrumentation and Measurement*, Vol. 61, no. 4, April 2012, pp. 903-911.
 [14] R. Colella et al., "Measurement Platform for Electromagnetic Characterization and Performance Evaluation of UHF RFID Tags", in *IEEE Transactions on instrumentation and measurement*, vol. 65, no. 4, January 2016, pp.905-914.
 [15] D. De Donno et al., "Differential RCS and Sensitivity Calculation of RFID Tags with Software-Defined Radio", in *Radio and Wireless Symposium*, 2012, pp. 9-12.
 [16] A. Briand et al., "Complete Software Defined RFID System Using GNU Radio", in *International Conference on RFID -Technologies and Applications*, 2012, pp. 287-291.
 [17] J.S. Moya et al., "A miniaturized low power radio frequency identification tag integrated in CMOS for biomedical applications", in *International Symposium on Instrumentation Systems, Circuits and Transducers (INSCIT)*, 2016, pp.10-13.
 [18] "Mosis integrated circuit fabrication service", <http://www.mosis.com/>.
 [19] F. L. Cabrera and F. R .de Sousa, "Contactless Characterization of a CMOS Integrated LC Resonator for Wireless Power Transferring", in *IEEE Microwave and Wireless Components Letters*, vol. 25, no.7, July 2015, pp. 475-477.
 [20] "Ettus Research", <https://www.ettus.com/>.
 [21] "GNU Radio: The free & open software radio ecosystem", <http://gnuradio.org>